

Adiabatic-impulse approximation for avoided level crossings: From phase-transition dynamics to Landau-Zener evolutions and back again

Bogdan Damski and Wojciech H. Zurek

Theory Division, Los Alamos National Laboratory, MS-B213, Los Alamos, New Mexico 87545, USA

(Received 5 December 2005; published 8 June 2006)

We show that a simple approximation based on concepts underlying the Kibble-Zurek theory of second order phase-transition dynamics can be used to treat avoided level crossing problems. The approach discussed in this paper provides an intuitive insight into quantum dynamics of two-level systems, and may serve as a link between the theory of dynamics of classical and quantum phase transitions. To illustrate these ideas we analyze dynamics of a paramagnet-ferromagnet quantum phase transition in the Ising model. We also present exact unpublished solutions of the Landau-Zener-like problems.

DOI: [10.1103/PhysRevA.73.063405](https://doi.org/10.1103/PhysRevA.73.063405)

PACS number(s): 32.80.Bx, 03.65.-w, 05.70.Fh

I. INTRODUCTION

Two-level quantum systems that undergo avoided level crossing play an important role in physics. Often they provide not only a qualitative description of system properties but also a quantitative one. The possibility for a successful two-level approximation arises in different physical systems, e.g., a single one-half spin; an atom placed in a resonant light; smallest quantum magnets; etc.

In this paper we focus on avoided level crossing dynamics in two-level quantum systems. Two interesting related extensions of the above-mentioned long list are the critical dynamics of quantum phase transitions [1–5] and adiabatic quantum computing [6]. In both of these cases (and, indeed, in all of the other applications of the avoided level crossing scenario) there are many more than two levels, but the essence of the problem can be still captured by the two-level, Landau-Zener type calculation.

Our interest in the Landau-Zener model originates also from its well-known numerous applications to different physical systems. In many cases there is a possibility of more general dependence of the relevant parameters (i.e., gap between the two levels on time) than in the original Landau-Zener treatment. This motivates our extensions in this paper of the level crossing dynamics to asymmetric level crossings and various power-law dependences. Appropriate variations of external parameters driving the Landau-Zener transition can allow for an experimental realization of these generalized Landau-Zener-like models in quantum magnets [7] and optical lattices [8].

We focus on evolutions that include both the adiabatic and diabatic (impulse) regime during a single sweep of a system parameter. For simplicity, we call these evolutions diabatic since we assume that they include a period of fast change of a system parameter. This is in contrast to adiabatic time evolutions induced by very slow parameter changes when the system never leaves the adiabatic regime. We will use a formalism proposed recently by one of us [9]. It originates from the so-called Kibble-Zurek (KZ) theory of topological defect production in the course of classical phase transitions [10,11], and works best for two-level systems. The two-level approximation was recently shown by Zurek *et al.* [2] and Dziarmaga [3] to be useful in studies of quantum phase tran-

sitions confirming earlier expectations—see Chap. 1.1 of [1,9]. Therefore we expect that the formalism presented here will provide a link between dynamical studies of classical and quantum phase transitions.

The present contribution extends the ideas presented in [9]. In particular, we have succeeded in replacing the fit to numerics used there for getting a free parameter of the theory, with a simple analytic calculation. We also show that the method of [9] can be successfully applied to a large class of two-level systems. Moreover, we present nontrivial exact analytic solutions for the Landau-Zener model and the relevant adiabatic-impulse approximations not published to date.

Section II presents basics of what we call the adiabatic-impulse approximation. Section III shows adiabatic-impulse, diabatic, and finally exact solutions to different versions of the Landau-Zener problem. In Sec. IV we discuss solutions for a whole class of two-level systems on the basis of adiabatic-impulse and diabatic schemes. Section V presents how results of Sec. III can be used to study quantum Ising model dynamics. Details of analytic calculations are in Appendix A (diabatic solutions), Appendix B (exact solutions of Landau-Zener problems), and Appendix C (adiabatic-impulse solution from Sec. IV).

II. ADIABATIC-IMPULSE APPROXIMATION

We will study dynamics of quantum systems by assuming that it includes *adiabatic* (no population transfer between instantaneous energy eigenstates) and *impulse* (no changes in the wave function except for an overall phase factor) stages only. The nature of this approach suggests the name *adiabatic-impulse* (AI) approximation. The AI approach originates from the Kibble-Zurek (KZ) theory of nonequilibrium classical phase transitions and we refer the reader to [9] for a detailed discussion of AI-KZ connections. Below, we summarize basic ideas of the KZ theory and the relevant assumptions used later on.

Second order phase transitions and avoided level crossings share one key distinguishing characteristic: in both cases sufficiently near the critical point (defined by the relaxation time or by the inverse of the size of the gap between the two levels) system “reflexes” become very bad. In phase

transitions this is known as “critical slowing down.”

In the treatment of the second order phase transitions this leads to the behavior where the state of the system can initially—in the adiabatic region far away from the transition—adjust to the change of the relevant parameter that induces the transition, but sufficiently close to the critical point its reflexes become too slow for it to react at all. As a consequence, a sequence of three regimes (adiabatic, impulse near the critical point, and adiabatic again on the other side of the transition) can be anticipated. In the second order phase transitions this allows one to employ a configuration dominated by the pretransition fluctuations to calculate salient features of the posttransition state of the order parameter (e.g., the density of topological defects). Key predictions of this KZ mechanism have been by now verified in numerical simulations [12,13] and more importantly in laboratory experiments [14–17].

The crux of this story is of course the moments when the transition from adiabatic to impulse and back to adiabatic behavior takes place. Assuming that the transition point is crossed at time $t=0$, this must happen around the instants $\pm\hat{t}$, where \hat{t} equals system relaxation time τ [11]. As the relaxation time depends on system parameter ε , which is changed as a function of time, one can write

$$\tau(\varepsilon(\hat{t})) = \hat{t}. \quad (1)$$

This basic equation proposed in [11] can be solved when dependence of τ on some measure of the distance from the critical point (e.g., relative temperature or coupling ε) is known. Assuming, e.g., $\tau = \tau_0/\varepsilon$ and $\varepsilon = t/\tau_Q$, where τ_Q , the “quench time,” contains information about how fast the system is driven through the transition, one arrives at $\tau_0/(\hat{t}/\tau_Q) = \hat{t}$. Hence the time \hat{t} at which the behavior switches between approximately adiabatic and approximately impulse is $\sqrt{\tau_0\tau_Q}$. Once this last “adiabatic” instant in the evolution of the system is known, interesting features of the posttransition state (such as the size of the regions $\hat{\xi}$ in which the order parameter is smooth) can be computed. Generalization to other universality classes is straightforward [11] and leads to

$$\hat{t} \sim \tau_Q^{1/(1+\nu)}, \quad \hat{\xi} \sim \tau_Q^{\nu/(1+\nu)}, \quad (2)$$

where z and ν are universal critical exponents (see, e.g., [12]).

In what follows we adopt this approach to quantum systems where dynamics can be approximated as an avoided level crossing (see Fig. 1). For simplicity we restrict ourselves to two-level systems that possess a single anticrossing (Fig. 1) in the excitation spectrum and a gap preferably going to $+\infty$ far away from the anticrossing. The latter condition guarantees that asymptotically the system enters the adiabatic regime.

The passage through avoided level crossing can be divided into an adiabatic and an impulse regime according to the size of the gap in comparison with the energy scale that characterizes the rate of the imposed changes in system Hamiltonian. If the gap is large enough the system is in the adiabatic regime, while when the gap is small it undergoes impulse time evolution as depicted in Fig. 1(b). The instants

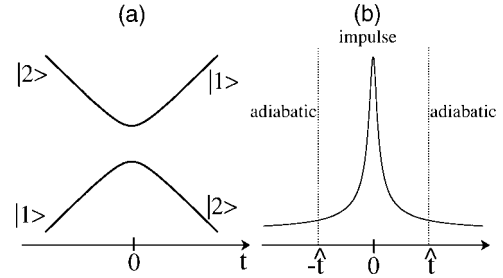


FIG. 1. (a) Structure of energy spectrum (parametrized by time) of a generic two-level system under consideration. Note the anti-crossing at $t=0$ and asymptotic form of eigenstates: $|1\rangle$, $|2\rangle$. (b) Adiabatic-impulse regimes in system dynamics. Compare it to a plot of relaxation time scale in the Kibble-Zurek theory [9,11]. Note that instants separating adiabatic and impulse regimes do not have to be placed symmetrically with respect to $t=0$ —see Sec. III A and Fig. 3.

$\pm\hat{t}$ are supposed to be such that the discrepancy between time dependent exact results and those coming from splitting of the evolution into only adiabatic and impulse parts is minimized. Therefore the AI approximation looks like a *time dependent variational method* where \hat{t} is a variational parameter while adiabatic-impulse assumptions provide a form of a variational wave function.

To make sure that assumptions behind the AI approach are correctly understood, let us consider time evolution of the system depicted in Fig. 1. Let the evolution start at $t_i \rightarrow -\infty$ from a ground state (GS) and last until $t_f \rightarrow +\infty$. The AI method assumes that the system wave function, $|\Psi(t)\rangle$, satisfies the following three approximations coming from passing through first adiabatic, then impulse and finally adiabatic regions:

$$t \in [-\infty, -\hat{t}]: |\Psi(t)\rangle \approx (\text{phase factor})|\text{GS at } t\rangle,$$

$$t \in [-\hat{t}, \hat{t}]: |\Psi(t)\rangle \approx (\text{phase factor})|\text{GS at } -\hat{t}\rangle,$$

$$t \in [\hat{t}, +\infty]: |\langle\Psi(t)|\text{GS at } t\rangle|^2 = \text{const.}$$

Finally, one needs to know how to get the instant \hat{t} . As proposed in [9], the proper generalization of Eq. (1) to the quantum case (after rescaling everything to dimensionless quantities) reads

$$\frac{1}{\text{gap}(\hat{t})} = \alpha\hat{t}, \quad (3)$$

where $\alpha = O(1)$ is a constant. Similarity between Eq. (3) and Eq. (1) suggests (in accord with physical intuition) that the quantum mechanical equivalent of the relaxation time scale is an inverse of the gap.

In this paper we give a simple and systematic way for (i) obtaining α analytically; and (ii) verification that Eq. (3) leads to correct results in the lowest nontrivial order. This method, illustrated on specific examples in Appendix A, is based on the observation that a time dependent Schrödinger equation can be solved exactly in the diabatic limit if one looks at the lowest nontrivial terms in expressions for exci-

tation amplitudes. This should be true even when getting an exact solution turns out to be very complicated or even impossible. After obtaining α this way, the whole AI approximation is complete in a sense that there are no free parameters, so its predictions can be rigorously checked by comparison to exact (either analytic or numeric) solution.

III. DYNAMICS IN THE LANDAU-ZENER MODEL

In this section we illustrate the AI approximation by considering the Landau-Zener model. In this way we supplement and extend the results of [9].

The Landau-Zener model, after rescaling all the quantities to dimensionless variables, is defined by the Hamiltonian:

$$H = \frac{1}{2} \begin{pmatrix} \frac{t}{\tau_Q} & 1 \\ 1 & -\frac{t}{\tau_Q} \end{pmatrix}, \quad (4)$$

where τ_Q is time independent and provides a time scale on which the system stays in the neighborhood of an anticrossing. As $\tau_Q \rightarrow 0$ the system undergoes diabatic time evolution, while $\tau_Q \gg 1$ means adiabatic evolution. There are two eigenstates of this model for any fixed time t : the ground state $|\downarrow(t)\rangle$ and the excited state $|\uparrow(t)\rangle$ given by

$$\begin{bmatrix} |\uparrow(t)\rangle \\ |\downarrow(t)\rangle \end{bmatrix} = \begin{pmatrix} \cos[\theta(t)/2] & \sin[\theta(t)/2] \\ -\sin[\theta(t)/2] & \cos[\theta(t)/2] \end{pmatrix} \begin{bmatrix} |1\rangle \\ |2\rangle \end{bmatrix}, \quad (5)$$

where $|1\rangle$ and $|2\rangle$ are time-independent basis states of the Hamiltonian (4); $\cos(\theta) = \varepsilon/\sqrt{1+\varepsilon^2}$; $\sin(\theta) = 1/\sqrt{1+\varepsilon^2}$;

$$\varepsilon = \frac{t}{\tau_Q}, \quad (6)$$

and $\theta \in [0, \pi]$. The gap in this model is

$$\text{gap} = \sqrt{1 + \varepsilon^2}.$$

The instant \hat{t} is obtained from Eq. (3):

$$\frac{1}{\sqrt{1 + \left(\frac{\hat{t}}{\tau_Q}\right)^2}} = \alpha \hat{t},$$

which leads to the following solution:

$$\hat{\varepsilon} = \frac{\hat{t}}{\tau_Q} = \frac{1}{\sqrt{2}} \sqrt{\left(1 + \frac{4}{(\alpha\tau_Q)^2}\right)^{1/2} - 1}. \quad (7)$$

Dynamics of the system is governed by the Schrödinger equation:

$$i \frac{d}{dt} |\Psi\rangle = H |\Psi\rangle,$$

and it will be assumed that evolution happens in the interval $[t_i, t_f]$.

As was discussed in [9], by using AI approximation one can easily arrive at the following predictions for the prob-

ability of finding the system in the excited state at $t_f \gg \hat{t}$.

(1) Time evolution starts at $t_i \ll -\hat{t}$ from the ground state

$$P_{AI} = |\langle \uparrow(\hat{t}) | \downarrow(-\hat{t}) \rangle|^2 = \frac{\hat{\varepsilon}^2}{1 + \hat{\varepsilon}^2}. \quad (8)$$

In this case the system undergoes in the AI scheme the adiabatic time evolution from t_i to $-\hat{t}$, then impulse one from $-\hat{t}$ to \hat{t} , and finally adiabatic from \hat{t} to $t_f \gg \hat{t}$.

(2) Time evolution starts at $t_i=0$ from the ground state

$$P_{AI} = |\langle \uparrow(\hat{t}) | \downarrow(0) \rangle|^2 = \frac{1}{2} \left(1 - \frac{1}{\sqrt{1 + \hat{\varepsilon}^2}} \right). \quad (9)$$

Now evolution is first impulse from $t=0$ to $t=\hat{t}$ and then adiabatic from \hat{t} to $t_f \gg \hat{t}$.

In the following we consistently denote excitation probability when the system evolves from $t_i \ll -\hat{t}$, $t_i=0$ by P , p , respectively. Additionally the subscript AI will be attached to predictions based on the AI approximation.

In the first case, the substitution of Eq. (7) into Eq. (8) leads to

$$P_{AI} = 1 - \alpha\tau_Q + \frac{(\alpha\tau_Q)^2}{2} - \frac{(\alpha\tau_Q)^3}{8} + O(\tau_Q^4). \quad (10)$$

Now we have to determine α . It turns out that it can be done by looking at the diabatic excitation probability. The proper expression and calculation can be found in Appendix A. Substituting $\eta=1/2$ into Eqs. (A6) and (A5) one gets that to the lowest nontrivial order $P_{AI} = 1 - \pi\tau_Q/2$, which implies that $\alpha = \pi/2$ and verifies Eq. (3) for this case. Note that the calculation leading to Eqs. (A5) and (A6) is not only much easier than determination of the exact LZ solution [18], but also really elementary. Therefore we expect that it can be done comparably easily for any model of interest.

Now we are ready to compare our AI approximation with α determined as above, to the exact result, i.e.,

$$P = \exp\left(-\frac{\pi\tau_Q}{2}\right). \quad (11)$$

First, the agreement between the exact and AI result is up to $O(\tau_Q^3)$, i.e., one order above the first nontrivial term. This is the advantage that the AI approximation provides over a simple diabatic approximation performed in Appendix A. Second, we see that the AI expansion contains the same powers of τ_Q as the diabatic (small τ_Q) expansion of the exact result. Third, Fig. 2 quantifies the discrepancies between exact, AI, and diabatic results. For the AI prediction, we plot in Fig. 2 instead of a Taylor series (10) the full expression evaluated in [9]

$$P_{AI} = \frac{2}{(\alpha\tau_Q)^2 + \alpha\tau_Q\sqrt{(\alpha\tau_Q)^2 + 4} + 2}, \quad (12)$$

with $\alpha = \pi/2$. As easily seen the AI approximation significantly outperforms a diabatic solution. In other words, the combination of AI simplification of dynamics and diabatic prediction for the purpose of getting the constant α leads to

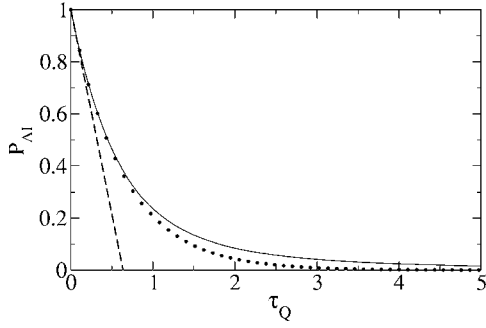


FIG. 2. Transition probability when the system starts time evolution from a ground state at $t_i \rightarrow -\infty$ and evolves to $t_f \rightarrow +\infty$. Dots: exact expression (11). Solid line: AI prediction (12) with $\alpha = \pi/2$ determined from the diabatic solution in Appendix A. Dashed thick line: lowest order diabatic result, $1 - \pi\tau_Q/2$, coming from Eqs. (A5) and (A6) with $\eta = 1/2$.

fully satisfactory results considering simplicity of the whole approach.

It is instructive to consider now separately three situations: (i) dynamics in a nonsymmetric avoided level crossing (Sec. III A); (ii) dynamics beginning at the anticrossing center (Sec. III B); and (iii) dynamics starting at $t_i \rightarrow -\infty$ but ending at the anticrossing center (Sec. III C). The first case will give us a hint whether $O(\tau_Q^3)$ agreement we have seen above is accidental and has something to do with the symmetry of the Landau-Zener problem. The second problem was preliminarily considered in [9], but without comparing the AI prediction to the exact analytic one being interesting on its own. Finally, the third problem is an example where AI approximation correctly suggests at a first sight unexpected symmetry between this problem and the one considered in Sec. III B.

A. Nonsymmetric Landau-Zener problem

We assume that system Hamiltonian is provided by the following expression:

$$H = \frac{1}{2} \begin{pmatrix} \frac{1}{\chi} \frac{t}{\tau_Q} & 1 \\ 1 & -\frac{1}{\chi} \frac{t}{\tau_Q} \end{pmatrix}, \quad \chi = \begin{cases} 1 & \text{for } t \leq 0 \\ \delta & \text{for } t > 0 \end{cases} \quad (13)$$

with $\delta > 0$ being the asymmetry parameter—see Fig. 3(a) for

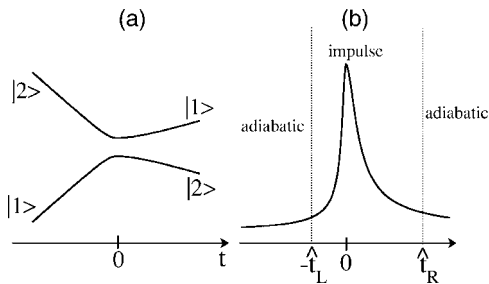


FIG. 3. The same as in Fig. 1 but for a nonsymmetric Landau-Zener problem with $\delta > 1$ —see Eq. (13).

schematic plot of the spectrum.

Once again, evolution starts at $t_i \rightarrow -\infty$ from a ground state. The exact expression for finding the system in the excited eigenstate at the end of time evolution ($t_f \rightarrow +\infty$) is

$$P = 1 - \frac{e^{-\pi(1+\delta)\tau_Q/8}}{2} \sinh\left(\frac{1}{4}\pi\tau_Q\delta\right) \times \left| \frac{\Gamma(1/2 + i\tau_Q\delta/8)}{\Gamma(1/2 + i\tau_Q/8)} + \sqrt{\frac{1}{\delta} \frac{\Gamma(1 + i\tau_Q\delta/8)}{\Gamma(1 + i\tau_Q/8)}} \right|^2, \quad (14)$$

and its derivation is presented in Appendix B. Naturally, for $\delta=1$, i.e., in a symmetric LZ problem, the expression (14) reduces to Eq. (11).

Now we would like to compare Eq. (14) to predictions coming from AI approximation. Due to asymmetry of the Hamiltonian the systems enter the impulse regime in the time interval $[-\hat{t}_L, \hat{t}_R]$ —see Fig. 3(b) for illustration of these concepts. The instants \hat{t}_L and \hat{t}_R are easily found in the same way as in the symmetric case. It is a straightforward exercise to verify that according to AI approximation, the probability of finding the system in the upper state is

$$P_{AI} = |\langle \downarrow(-\hat{t}_L) | \uparrow(\hat{t}_R) \rangle|^2. \quad (15)$$

To simplify comparison between exact (14) and approximate (15) excitation probabilities we will present their diabatic Taylor expansions:

$$P_{AI} = 1 - \frac{1}{4}(1 + \sqrt{\delta})^2 \alpha \tau_Q + \frac{1}{16}(1 + \delta)(1 + \sqrt{\delta})^2 (\alpha \tau_Q)^2 + O(\tau_Q^3). \quad (16)$$

Determination of the constant α is easy and is presented in Appendix A. By putting $\eta = 1/2$ into Eqs. (A6) and (A10), one gets that $\alpha = \pi/2$.

The AI prediction can be easily compared to the exact result (14) after series expansion

$$P = 1 - \frac{\pi}{8}(1 + \sqrt{\delta})^2 \tau_Q + \frac{\pi^2}{64}(1 + \delta)(1 + \sqrt{\delta})^2 \tau_Q^2 + O(\tau_Q^3).$$

This comparison shows that once again there is perfect matching between exact and AI description up to $O(\tau_Q^3)$, i.e., one order better than the simple diabatic approximation from Appendix A, despite the fact that we deal now with a nonsymmetric LZ problem. Moreover, the constant α is the same in symmetric and nonsymmetric cases. Finally the same powers of τ_Q show up in both exact and AI results.

The nonsymmetric Landau-Zener model is also interesting in the light of a recent paper [19], where it is argued that the final state of the system that passed through a classical phase transition point is determined by details of dynamics after phase transition. In our system, there are two different quench rates: τ_Q before the transition and $\tau'_Q = \tau_Q \delta$ after the transition. Substitution of $\delta = \tau'_Q / \tau_Q$ into Eq. (14) shows that the final state of the nonsymmetric Landau-Zener model expressed in terms of the excitation probability depends on both τ_Q and τ'_Q , so that it behaves differently than the system described in [19].

B. Landau-Zener problem when time evolution starts at the anticrossing center

Now we consider the LZ problem characterized by Hamiltonian (4) in the case when time evolution starts from the ground state at the anticrossing center, i.e., $t_i=0$. It means that $|\Psi(0)\rangle \propto (|1\rangle - |2\rangle)/\sqrt{2}$. Excitation probability at $t_f \rightarrow +\infty$ equals exactly (see Appendix B)

$$p = 1 - \frac{2}{\pi\tau_Q} \sinh\left(\frac{\pi\tau_Q}{4}\right) e^{-\pi\tau_Q/8} \left| \Gamma\left(1 + \frac{i\tau_Q}{8}\right) + e^{i\pi/4} \sqrt{\frac{\tau_Q}{8}} \Gamma\left(\frac{1}{2} + \frac{i\tau_Q}{8}\right) \right|^2. \quad (17)$$

From the point of view of AI approximation the evolution is now simplified by assuming that it is impulse from $t_i=0$ to \hat{t} and then adiabatic from \hat{t} to $t_f \rightarrow +\infty$. This case was discussed in [9], and it was shown that substitution of Eq. (7) into Eq. (9) leads to a simple expression

$$p_{AI} = \frac{1}{2} - \frac{1}{2} \sqrt{1 - \frac{2}{(\alpha\tau_Q)^2 + \alpha\tau_Q\sqrt{(\alpha\tau_Q)^2 + 4} + 2}}, \quad (18)$$

expanding it into diabatic series one gets

$$p_{AI} = \frac{1}{2} - \frac{1}{2} \sqrt{\alpha\tau_Q} + \frac{1}{8} (\alpha\tau_Q)^{3/2} + O(\tau_Q^{5/2}). \quad (19)$$

Determination of a constant α is straightforward (see Appendix A). Putting $\eta=1/2$ into Eqs. (A8) and (A9) one easily gets $\alpha=\pi/4$ and confirms that the first nontrivial term in Eq. (19) is indeed $\propto\sqrt{\tau_Q}$. This value of α (≈ 0.785) is in agreement with the numerical fit done in [9] where optimal α was found to be equal to 0.77. Small disagreement comes from the fact that now we use just the $\frac{1}{2} - \frac{1}{2}\sqrt{\alpha\tau_Q}$ part for getting α , which is equivalent to making the fit to exact results in the limit of $\tau_Q \ll 1$. In [9] the fit of the whole expression (18) in the range of $0 < \tau_Q < 6$ was done.

Having the exact solution (17) at hand, we can verify rigorously accuracy of Eqs. (18) and (19) with the choice of $\alpha=\pi/4$. Expanding Eq. (17) into diabatic series one gets

$$p = \frac{1}{2} - \frac{\sqrt{\pi}}{4} \sqrt{\tau_Q} + \frac{\pi^{3/2}}{64} \left(2 - \frac{4 \ln 2}{\pi}\right) \tau_Q^{3/2} + O(\tau_Q^{5/2}). \quad (20)$$

As expected the first nontrivial term is in perfect agreement with Eq. (19) once $\alpha=\pi/4$. On the other hand, the term proportional to $\tau_Q^{3/2}$ is about 10% off. Indeed, after substitution $\alpha=\pi/4$ into Eq. (19) one gets the third term equal to $\pi^{3/2}\tau_Q^{3/2}/64$, which has to be compared to $\approx 1.1\pi^{3/2}\tau_Q^{3/2}/64$ from Eq. (20). It shows that the AI approximation in this case does not predict exactly higher nontrivial terms in the diabatic expansion.

Nonetheless, expression (18) works much better than the above comparison suggests. It not only significantly outperforms the lowest order diabatic expansion, $\frac{1}{2} - \frac{1}{4}\sqrt{\pi\tau_Q}$, but also beautifully fits to the exact result pretty far from the $\tau_Q \ll 1$ regime. Figure 4 leaves no doubt about these statements. It suggests that AI predictions should be compared to exact results not only term by term as in the diabatic expansion, but also in a full form.

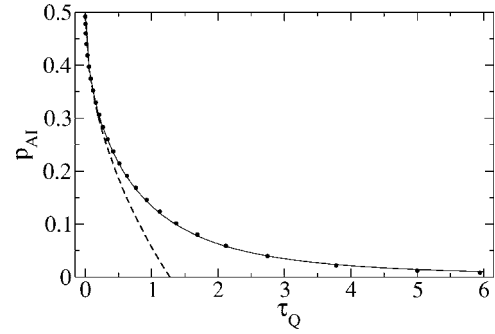


FIG. 4. Transition probability when the system starts time evolution at the anticrossing center from a ground state and evolves to $t_f \rightarrow +\infty$. Dots: exact expression (17). Solid line: AI prediction (18) with $\alpha=\pi/4$ determined from the diabatic solution in Appendix A. Dashed thick line: lowest order diabatic prediction $1/2 - \sqrt{\pi\tau_Q}/4$ coming from Eqs. (A8) and (A9) with $\eta=1/2$.

C. One-half of Landau-Zener evolution

In this section we consider exactly one-half of the LZ problem. Namely, we take the Hamiltonian (4) and evolve the system to the anticrossing center, $t_f=0$, while starting from the ground state at $t_i \rightarrow -\infty$.

Let us see what the AI approximation predicts for excitation probability of the system at $t_f=0$. According to AI, evolution is adiabatic in the interval $[-\infty, -\hat{t}]$ and then impulse in time range $[-\hat{t}, 0]$. It implies that

$$|\langle \uparrow(0) | \Psi(0) \rangle|^2 \approx |\langle \uparrow(0) | \Psi(-\hat{t}) \rangle|^2 \approx |\langle \uparrow(0) | \downarrow(-\hat{t}) \rangle|^2.$$

A simple calculation then shows that

$$P_{AI} = |\langle \uparrow(0) | \downarrow(-\hat{t}) \rangle|^2 = \frac{1}{2} \left(1 - \frac{1}{\sqrt{1 + \hat{\epsilon}^2}}\right). \quad (21)$$

A quick look at Eq. (9) shows that the excitation probability for one-half of the Landau-Zener problem is supposed to be, according to the AI scheme, equal to the excitation probability when the system starts from the anticrossing and evolves toward $t_f \rightarrow +\infty$.

To check that prediction we have solved the one-half LZ model exactly, see Appendix B, and found that indeed both probabilities are exactly the same, so the AI approximation provides us here with a prediction that is correct not only qualitatively but also quantitatively.

IV. DYNAMICS IN A GENERAL CLASS OF QUANTUM TWO-LEVEL SYSTEMS

To test predictions coming from the AI approximation on two-level systems different than the classic Landau-Zener model, we consider in this section dynamics induced by the Hamiltonian

$$H = \frac{1}{2} \begin{pmatrix} \operatorname{sgn}(t) \left| \frac{t}{\tau_Q} \right|^{\eta(1-\eta)} & 1 \\ 1 & -\operatorname{sgn}(t) \left| \frac{t}{\tau_Q} \right|^{\eta(1-\eta)} \end{pmatrix}, \quad (22)$$

where $\eta \in (0, 1)$ is a constant parameter (when $\eta=1/2$ the system reduces to the Landau-Zener model). The eigenstates of Hamiltonian (22) are expressed by formula (5) with

$$\cos(\theta) = \frac{\operatorname{sgn}(t) \left| \frac{t}{\tau_Q} \right|^{\eta(1-\eta)}}{\sqrt{1 + \left| \frac{t}{\tau_Q} \right|^{2\eta(1-\eta)}}},$$

and

$$\sin(\theta) = \frac{1}{\sqrt{1 + \left| \frac{t}{\tau_Q} \right|^{2\eta(1-\eta)}}}.$$

Extending the notation of Sec. III to the system (22) one has to replace definition (6) by

$$\varepsilon = \operatorname{sgn}(t) \left| \frac{t}{\tau_Q} \right|^{\eta(1-\eta)}$$

and then expressions (8) and (9) providing excitation probabilities are valid also for the model (22).

The instant \hat{t} for the Hamiltonian (22) is determined by the following version of Eq. (3):

$$\frac{1}{\sqrt{1 + \left| \frac{\hat{t}}{\tau_Q} \right|^{2\eta(1-\eta)}}} = \alpha \hat{t}. \quad (23)$$

It seems to be impossible to obtain the solution of Eq. (23) exactly. Fortunately, a diabatic perturbative expansion for \hat{t} can be found—see Appendix C. Once the diabatic expansion of \hat{t} is known, we can present different predictions about dynamics of the model (22).

First, we consider transitions starting from a ground state at $t_i \rightarrow -\infty$ and lasting until $t_f \rightarrow +\infty$. Using the results of Appendix C one gets the following expression for the excitation probability:

$$\begin{aligned} P_{AI} &= \frac{\hat{\varepsilon}^2}{1 + \hat{\varepsilon}^2} = 1 - (\alpha\tau_Q)^{2\eta} + (1-\eta)(\alpha\tau_Q)^{4\eta} \\ &\quad - \frac{1}{2}(1-\eta)(2-3\eta)(\alpha\tau_Q)^{6\eta} + \frac{1}{3}(1-\eta)(1-2\eta) \\ &\quad \times (3-4\eta)(\alpha\tau_Q)^{8\eta} + O(\tau_Q^{10\eta}). \end{aligned} \quad (24)$$

This result is equivalent to Eq. (10) when one puts $\eta=1/2$. The constant α was found in Appendix A from the diabatic solution and equals Eq. (A6)

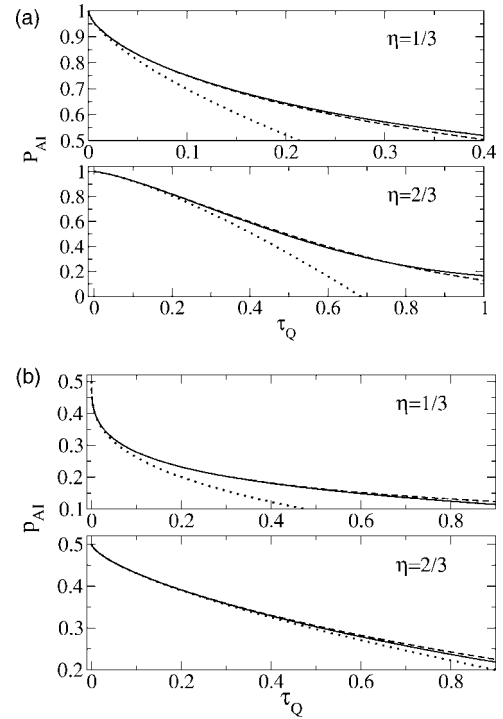


FIG. 5. Numerics: bold dashed line, AI approximation: solid line, and lowest order exact diabatic expansion (Appendix A): dotted line. (a) Evolution starts from $t_i \rightarrow -\infty$. (b) Evolution starts from $t_i=0$. In both (a) and (b) evolution ends in $t_f \rightarrow +\infty$.

$$\alpha = (1-\eta)\Gamma(1-\eta)^{1/\eta}.$$

The exponent 2η in the lowest order term in Eq. (24) was positively verified (Appendix A). Additionally, we have performed numerical simulations for $\eta=1/3, 2/3, 3/4, 5/6$. A fit to numerics in the range of $\tau_Q \ll 1$ has confirmed both the exponent 2η and the value of α . The comparison between the AI prediction for $\eta=1/3, 2/3$ and numerics is presented in Fig. 5(a). The lack of exact solution for this problem does not allow us a more systematic analytic investigation of the AI approximation in this case. Nonetheless, a good agreement between AI and numerics is easily noticed. Once again, the AI prediction outperforms the lowest order diabatic expansion.

As before, we would like to consider transitions starting from the anticrossing center, i.e., $t_i=0$. In this case the excitation probability equals

$$\begin{aligned} P_{AI} &= \frac{1}{2} \left(1 - \frac{1}{\sqrt{1 + \hat{\varepsilon}^2}} \right) = \frac{1}{2} - \frac{1}{2} (\alpha\tau_Q)^\eta + \frac{1}{4} (1-\eta) \\ &\quad \times (\alpha\tau_Q)^{3\eta} - \frac{1}{16} (1-\eta)(3-5\eta)(\alpha\tau_Q)^{5\eta} + O(\tau_Q^{7\eta}). \end{aligned} \quad (25)$$

As above, the diabatic calculation of Appendix A verifies the exponent of the first nontrivial term in Eq. (25) and provides us with the following prediction for α (A9)

$$\alpha = (1 - \eta)\Gamma(1 - \eta)^{1/\eta} \cos\left(\frac{\pi}{2}\eta\right)^{1/\eta}.$$

After setting $\eta=1/2$ formula (25) becomes the same as Eq. (19). Due to the lack of exact results we have carried out numerical simulations for $\eta=1/3, 2/3, 3/4, 5/6$. As expected, this calculation has confirmed that the exponent of τ_Q is indeed η for small τ_Q and that α is provided by Eq. (A9). The AI approximation vs numerics and diabatic expansion for $\eta=1/3, 2/3$ is presented in Fig. 5(b). Once again an overall agreement is strikingly good.

V. QUANTUM PHASE TRANSITION IN ISING MODEL VS ADIABATIC-IMPULSE APPROACH

In this section we will illustrate how ideas coming from the adiabatic-impulse approach can be used in studies of dynamics of quantum phase transition. As an example we choose the quantum Ising model recently considered in this context [2–4]. The quantum Ising model is defined by the following Hamiltonian

$$H = - \sum_{n=1}^N (g\sigma_n^x + \sigma_n^z \sigma_{n+1}^z), \quad (26)$$

where N is the number of spins. The quantum phase transition in this model is driven by the change of a dimensionless coupling g . The transition point between paramagnetic phase ($g > 1$) and ferromagnetic one ($0 \leq g < 1$) is at $g = 1$. To study dynamics of Eq. (26) one assumes that the system evolves from time $t' = -\infty$ to time $t' = 0$, and takes

$$g = - \frac{t'}{\tau_Q},$$

where τ_Q provides a quench rate. The quantity of interest is density of topological defects (kinks) after completion of the transition, i.e., at $g=0$. It equals [3]

$$n = \lim_{N \rightarrow +\infty} \left\langle \frac{1}{2N} \sum_{n=1}^{N-1} (1 - \sigma_n^z \sigma_{n+1}^z) \right\rangle. \quad (27)$$

The quantum Ising model obviously possesses 2^N different energy eigenstates so it seems to be hopeless to expect that the two-level approximation would be sufficient. Therefore it is a remarkable result of Dziarmaga [3] that dynamics in this system can be exactly described by a series of uncoupled Landau-Zener systems. Due to lack of space, we refer the reader to [3], and present just the main results and their AI equivalents.

The density of defects (27) in Dziarmaga's notation reads as

$$n = \frac{1}{2\pi} \int_{-\pi}^{\pi} dk p_k, \quad (28)$$

where p_k 's are defined as

$$p_k = |\cos(k/2)u_k(t'=0) - \sin(k/2)v_k(t'=0)|^2, \quad (28)$$

with u_k, v_k satisfying the following Landau-Zener system:

$$i \frac{d}{dt} \begin{pmatrix} v_k \\ u_k \end{pmatrix} = \frac{1}{2} \begin{pmatrix} t & 1 \\ \tau_Q & -t \end{pmatrix} \begin{pmatrix} v_k \\ u_k \end{pmatrix},$$

$$t = 4(t' + \tau_Q \cos k) \sin k,$$

$$\tau_Q = 4\tau_Q' \sin^2 k, \quad (29)$$

where t' changes from $-\infty$ to 0. The initial conditions for that LZ system are the following:

$$|u_k(t' = -\infty)| = 1, \quad v_k(t' = -\infty) = 0. \quad (30)$$

Due to the symmetry of the whole problem, it is possible to show that $p_k \equiv p_{-k}$, and therefore it is sufficient to restrict to $k \geq 0$ from now on.

Evolution in Eq. (29) lasts from $t_i = -\infty$ to $t_f = 2\tau_Q' \sin(2k)$. Since obviously t_f does not go to $+\infty$, it is important to determine where t_f is placed with respect to $\pm \hat{t}$.

We solve the equation $\hat{t} = |t_f|$ (where we substitute $k = k_c$). After using Eq. (7) with $\alpha = \pi/2$ and simple algebra one arrives at

$$\frac{1}{\sqrt{2}} \sqrt{\left(1 + \frac{4}{(\pi\tau_Q/2)^2}\right)^{1/2} - 1} = \left| \frac{\cos k_c}{\sin k_c} \right|,$$

which leads to the result

$$\sin^2 k_c = 1 - \frac{1}{4\pi^2 \tau_Q'^2}.$$

Defining k_c to be between 0 and $\pi/2$ and doing some additional easy calculations one gets that when $\tau_Q' > \frac{1}{2\pi}$ we have: (i) $t_f \geq \hat{t}$ for $k \in [0, k_c]$; (ii) $-\hat{t} < t_f < \hat{t}$ for $k \in (k_c, \pi - k_c)$; and (iii) $t_f \leq -\hat{t}$ for $k \in [\pi - k_c, \pi]$. Moreover, when $\tau_Q' < \frac{1}{2\pi}$ one can show that $|t_f| < \hat{t}$ for any k 's of interest. It means that the evolution ends in the impulse regime for small enough τ_Q' .

Now, as in [2–4], we consider adiabatic time evolutions of the Ising model. In our scheme it clearly corresponds to $\tau_Q' \gg \frac{1}{2\pi}$. As the system undergoes slow evolution it is safe to assume that only long wavelength modes are excited, which means that $k \ll \pi/4$ are of interest. This allows us to approximate $\sin k \sim k$ and $\cos k \sim 1$, which implies that Eq. (28) turns into $p_k \approx |u_k(t_f)|^2$ and that

$$n \approx \frac{1}{\pi} \int_0^\epsilon dk |u_k(t_f)|^2,$$

with $\epsilon \ll \pi/4$. Since $k \in [0, \epsilon]$ corresponds to the above-mentioned (i) case, $t_f > \hat{t}$, the AI approximation says that $|u_f(t_f)| \approx |u_f(+\infty)|$. Initial conditions (30) mean that the system starts time evolution at $t = -\infty$ from *excited* state and we are interested in the probability of finding it in the *ground* state at t_f . Elementary algebra based on AI approximation shows that this probability equals

$$|u_k(t_f)|^2 = |\langle \uparrow(-\hat{v}) | \downarrow(\hat{v}) \rangle|^2 = |\langle \downarrow(-\hat{v}) | \uparrow(\hat{v}) \rangle|^2.$$

Therefore it is provided by Eqs. (8) and (12). For any fixed ϵ consistent with lowest order approximation of $\sin k$ and $\cos k$ one gets

$$n \cong 0.172 \frac{1}{\sqrt{2\tau'_Q}}, \quad (31)$$

where the prefactor was found from expansion of the integral into $1/\sqrt{\tau'_Q}$ adiabatic series with $\tau'_Q \rightarrow +\infty$ at fixed ϵ . In the derivation of this result $\sin^2 k$ in the expression for τ_Q was approximated by k^2 .

First of all, the prediction (31) provides correct scaling of defect density with τ'_Q . The prefactor, 0.172, has to be compared to $\frac{1}{2\pi} \approx 0.16$ (exact result from [3] and numerical estimation from [2]) or 0.18 (approximate result from [4]). Our prefactor matches these results remarkably closely concerning simplicity of the whole AI approximation. Slight overestimation of the prefactor in comparison to exact result comes from the fact that AI transition probability, Eq. (12), overestimates the exact result, Eq. (11), for large τ_Q 's (Fig. 2). It is interesting to note that in the Kibble-Zurek scheme used for description of classical phase transitions an overestimation of defect density is usually of the order of $O(1)$ [2,12,13], while here discrepancy is smaller than 10%.

Therefore the AI approximation provides us with two predictions concerning dynamics of the quantum Ising model: (i) it estimates when evolution ends in the asymptotic limit; and (ii) it correctly predicts the scaling exponent and number of defects produced during adiabatic transitions. The part (ii) can be calculated exactly in the quantum Ising model (26). Nonetheless, in other systems undergoing quantum phase transition the two-level simplification might be too difficult for exact analytic treatment, e.g., as in the system governed by Eq. (22). Then the AI analysis might be the only analytic approach working beyond the lowest order diabatic expansion. Besides that the AI approach provides us with a quite intuitive description of system dynamics, which is of interest in its own. Especially when one looks at connections between classical and quantum phase transitions.

VI. SUMMARY

We have shown that the adiabatic-impulse approximation, based on the ideas underlying the Kibble-Zurek mechanism [10,11], provides good quantitative predictions concerning diabatic dynamics of two-level Landau-Zener-like systems. After supplementing the splitting of the evolution into adiabatic and impulse regimes by the exact lowest order diabatic calculation, the whole approach is complete and can be in principle applied to different systems possessing anticrossings, e.g., those lacking exact analytic solution as the model (22). We expect that the AI approach will provide the link between dynamics of classical and quantum phase transition thanks to usage of the same terminology and similar assumptions.

We also expect that different variations of the classic Landau-Zener system discussed in this paper can be experi-

mentally realized in the setting where the sweep rate can be manipulated. Indeed, the model (22) arises once a proper nonlinear change of external system parameter is performed. The experimental access to studies of the nonsymmetric Landau-Zener model can be obtained by change of the sweep rate after passing an anticrossing center. The case of evolution starting from or ending at the anticrossing center can also be subjected to experimental investigations, e.g., in a beautiful system consisting of the smallest available quantum magnets (cold Fe_8 clusters) [7].

ACKNOWLEDGMENTS

We are grateful to Uwe Dörner for collaboration on the nonsymmetric Landau-Zener problem, and Jacek Dziarmaga for comments and useful suggestions on the manuscript. This work was supported by the U.S. Department of Energy, National Security Agency, and the ESF COSLAB program.

APPENDIX A: EXACT DIABATIC EXPRESSIONS FOR TRANSITION PROBABILITIES

We would like to provide lowest order exact expressions for transition probabilities in a class of two-level systems described by the Hamiltonian (22).

First, we express the wave function as

$$|\Psi(t)\rangle = C_1(t) \exp\left(\frac{-i(1-\eta)|t|^{1/(1-\eta)}}{2\tau_Q^{\eta/(1-\eta)}}\right) |1\rangle + C_2(t) \exp\left(\frac{i(1-\eta)|t|^{1/(1-\eta)}}{2\tau_Q^{\eta/(1-\eta)}}\right) |2\rangle, \quad (\text{A1})$$

where exponentials are $\mp i \int dt \text{sgn}(t) |t/\tau_Q|^{\eta/(1-\eta)}/2$. Within this representation dynamics governed by the Hamiltonian (22) reduces to

$$i\dot{C}_1(t) = \frac{C_2(t)}{2} \exp\left(\frac{i(1-\eta)|t|^{1/(1-\eta)}}{\tau_Q^{\eta/(1-\eta)}}\right), \quad (\text{A2})$$

$$i\dot{C}_2(t) = \frac{C_1(t)}{2} \exp\left(\frac{-i(1-\eta)|t|^{1/(1-\eta)}}{\tau_Q^{\eta/(1-\eta)}}\right). \quad (\text{A3})$$

(i) *Time evolution starting from the ground state at $t_i \rightarrow -\infty$:* We would like to integrate Eq. (A3) from $-\infty$ to $+\infty$. The initial condition is such that $C_1(-\infty)=1$ and $C_2(-\infty)=0$. The simplification comes when one assumes a very fast transition, i.e., $\tau_Q \rightarrow 0$. Then it is clear that $C_1(t)=1+O(\tau_Q^\beta)$ with some $\beta>0$. Putting such $C_1(t)$ into Eq. (A3) one gets

$$C_2(+\infty) = \frac{1}{2i} \tau_Q^\eta \int_{-\infty}^{+\infty} dx \exp[-i(1-\eta)|x|^{1/(1-\eta)}] + (\text{higher order terms in } \tau_Q), \quad (\text{A4})$$

which after some algebra results in

$$P = |C_1(+\infty)|^2 = 1 - |C_2(+\infty)|^2 = 1 - (\alpha\tau_Q)^{2\eta} + (\text{higher order terms in } \tau_Q), \quad (\text{A5})$$

where

$$\alpha = (1 - \eta)\Gamma(1 - \eta)^{1/\eta}. \quad (\text{A6})$$

(ii) *Time evolution starting from the ground state at $t_i=0$ (anticrossing center):* Since the initial wave function is $(|1\rangle - |2\rangle)/\sqrt{2}$ we have $C_1(0)=1/\sqrt{2}$ and $C_2(0)=-1/\sqrt{2}$ and we evolve the system until $t_f \rightarrow +\infty$ with the Hamiltonian (22). For fast transitions one has that $C_1(t)=1/\sqrt{2} + O(\tau_Q^\beta)$, where $\beta > 0$ is some constant. Integrating Eq. (A3) from 0 to $+\infty$ one gets

$$C_2(+\infty) + \frac{1}{\sqrt{2}} = \frac{\tau_Q^\eta}{2\sqrt{2}i} \int_0^{+\infty} dx \exp[-i(1-\eta)x^{1/(1-\eta)}] + (\text{higher order terms in } \tau_Q), \quad (\text{A7})$$

which can be easily shown to lead to

$$p = |C_1(+\infty)|^2 = 1 - |C_2(+\infty)|^2 = \frac{1}{2} - \frac{1}{2}(\alpha\tau_Q)^\eta + (\text{higher order terms in } \tau_Q), \quad (\text{A8})$$

where

$$\alpha = (1 - \eta)\Gamma(1 - \eta)^{1/\eta} \cos\left(\frac{\pi}{2}\eta\right)^{1/\eta}. \quad (\text{A9})$$

(iii) *Time evolution from $t_i \rightarrow -\infty$ to $t_f \rightarrow +\infty$ in the nonsymmetric LZ model:* We assume that the Hamiltonian is given by Eq. (22) for $t \leq 0$, while for $t > 0$ it is given by Eq. (22) with τ_Q exchanged by $\tau_Q\delta$ where $\delta > 0$ is the asymmetry constant—see Eq. (13) for the $\eta=1/2$ case. Integration of Eq. (A3) separately in the intervals $[-\infty, 0]$ and $[0, +\infty]$ leads to the following prediction:

$$P = |C_1(+\infty)|^2 = 1 - |C_2(+\infty)|^2 = 1 - \frac{1}{4}(1 + \delta\eta)^2(\alpha\tau_Q)^{2\eta} + (\text{higher order terms in } \tau_Q), \quad (\text{A10})$$

with α given by Eq. (A6).

APPENDIX B: EXACT SOLUTIONS OF THE LANDAU-ZENER SYSTEM

In this Appendix we present derivation of exact solutions of the Landau-Zener problem that are used in the main part of the paper. The general exact solution for the Landau-Zener model evolving according to Hamiltonian (4) was first discussed in [18] and then elaborated in a number of papers, e.g., [20]. Here we will use that general solution for getting predictions about different time evolutions. The problem is simplified by writing the wave function as Eq. (A1) with $\eta = 1/2$. Then one arrives at the equations (A2) and (A3) once again with $\eta=1/2$. Combining the latter ones with the substitution

$$U_2(t) = C_2(t)e^{it^2/(4\tau_Q)}$$

one gets

$$\ddot{U}_2(z) + \left(k - \frac{z^2}{4} + \frac{1}{2}\right)U_2(z) = 0,$$

where

$$k = \frac{i\tau_Q}{4}, \quad z = \frac{t}{\sqrt{\tau_Q}}e^{-i\pi/4}. \quad (\text{B1})$$

The general solution of this equation is expressed in terms of linearly independent Weber functions $D_{-k-1}(\pm iz)$ [18,21]. By combining this observation with a $\eta=1/2$ version of Eq. (A3) one gets

$$|\Psi(t)\rangle = 2i \left[\partial_t - \frac{it}{2\tau_Q} \right] [aD_{-k-1}(iz) + bD_{-k-1}(-iz)]|1\rangle + [aD_{-k-1}(iz) + bD_{-k-1}(-iz)]|2\rangle, \quad (\text{B2})$$

where z is defined in Eq. (B1). Though there is a simple one-to-one correspondence between z and t , we will use both z and t in different expressions to shorten notation.

To determine constants a and b in different cases one has to know the following properties of Weber functions [21]. First, $\forall |\arg(s)| < 3\pi/4$ one has

$$D_m(s) = e^{-s^2/4} s^m [1 + O(s^{-2})]. \quad (\text{B3})$$

Second, $\forall -5\pi/4 < \arg(s) < -\pi/4$

$$D_m(s) = e^{-im\pi} D_m(-s) + \frac{\sqrt{2\pi}}{\Gamma(-m)} e^{-i(m+1)\pi/2} D_{-m-1}(is). \quad (\text{B4})$$

Third, as $s \rightarrow 0$ one has

$$D_m(s) = 2^{m/2} \frac{\sqrt{\pi}}{\Gamma(1/2 - m/2)} + O(s). \quad (\text{B5})$$

Finally,

$$\frac{d}{ds} D_m(s) = m D_{m-1}(s) - \frac{1}{2} s D_m(s). \quad (\text{B6})$$

(i) *Exact solution of nonsymmetric LZ problem:* The evolution starts at $t_i \rightarrow -\infty$, i.e., up to a phase factor $|\Psi(-\infty)\rangle \sim |1\rangle$. The Hamiltonian is given by Eq. (13). Using Eqs. (B3), (B4), and (B6) one finds that $a=0$ and $b = \sqrt{\tau_Q} \exp(-\pi\tau_Q/16)/2$. Substituting them into Eq. (B2) results in

$$|\Psi(t \leq 0)\rangle = e^{-\pi\tau_Q/16} e^{i3\pi/4} [(k+1)D_{-k-2}(-iz) - izD_{-k-1}(-iz)]|1\rangle + \frac{\sqrt{\tau_Q}}{2} e^{-\pi\tau_Q/16} D_{-k-1}(-iz)|2\rangle. \quad (\text{B7})$$

Using Eq. (B5) one finds that this solution at $t=0$ becomes

$$|\Psi(0)\rangle = e^{-\pi\tau_Q/16} e^{i3\pi/4} \frac{\sqrt{\pi} 2^{-k/2}}{\Gamma(1/2 + k/2)} |1\rangle + \frac{\sqrt{\tau_Q}}{2} e^{-\pi\tau_Q/16} \sqrt{\frac{\pi}{2}} \frac{2^{-k/2}}{\Gamma(1 + k/2)} |2\rangle. \quad (\text{B8})$$

For $t > 0$ the Hamiltonian changes its form, see Eq. (13), and one has to match Eq. (B8) with Eq. (B2) having τ_Q replaced by $\tau_Q\delta$. Substitution of

$$a = \frac{e^{-\pi\tau_Q/16}}{4} 2^{-k(1-\delta)/2} \sqrt{\tau_Q} \delta \left[\frac{\Gamma(1+k\delta/2)}{\Gamma(1+k/2)} \sqrt{\frac{1}{\delta}} - \frac{\Gamma(1/2+k\delta/2)}{\Gamma(1/2+k/2)} \right],$$

$$b = \frac{e^{-\pi\tau_Q/16}}{4} 2^{-k(1-\delta)/2} \sqrt{\tau_Q} \delta \left[\frac{\Gamma(1+k\delta/2)}{\Gamma(1+k/2)} \sqrt{\frac{1}{\delta}} + \frac{\Gamma(1/2+k\delta/2)}{\Gamma(1/2+k/2)} \right],$$

into Eq. (B2) gives the wave function $|\Psi(t \geq 0)\rangle$. Taking one minus squared modulus of the amplitude of finding the system in the state $|2\rangle$ one obtains the excitation probability of the system at $t_f \rightarrow +\infty$ in the form (14).

(ii) *Exact solution of LZ problem when evolution starts from a ground state at anticrossing center:* The Hamiltonian of the system is given by Eq. (4) and we look for a solution that starts at $t=0$ from the (ground) state: $|\Psi(0)\rangle = (|1\rangle - |2\rangle)/\sqrt{2}$. The constants a and b from Eq. (B2) turn out to be equal to

$$a = \frac{2^{k/2} \Gamma(1/2+k/2) e^{i\pi/4} \sqrt{\tau_Q}}{4\sqrt{2}\pi} - 2^{k/2} \frac{\Gamma(1+k/2)}{2\sqrt{\pi}},$$

$$b = -\frac{2^{k/2} \Gamma(1/2+k/2) e^{i\pi/4} \sqrt{\tau_Q}}{4\sqrt{2}\pi} - 2^{k/2} \frac{\Gamma(1+k/2)}{2\sqrt{\pi}}.$$

Having this at hand, it is straightforward to show that one minus squared modulus of the amplitude of finding the system in the state $|2\rangle$ at $t_f \rightarrow +\infty$, i.e., excitation probability, equals Eq. (17).

(iii) *One-half of the Landau-Zener problem:* The excitation probability of the system that started time evolution at $t_i = -\infty$ from ground state, and stopped evolution at $t_f = 0$, turns out to be equal to Eq. (17). The simplest way to prove it comes from an observation that this probability equals one minus the squared overlap between the state $(|1\rangle - |2\rangle)/\sqrt{2}$ and Eq. (B8). Then, straightforward calculation leads immediately to expression (17).

APPENDIX C: SOLUTION OF EQ. (23)

Equation (23) can be solved in the following recursive way. First, one introduces new variables:

$$x = \left(\frac{\hat{t}}{\tau_Q} \right)^2, \quad \beta = \frac{1}{\alpha^2 \tau_Q^2}. \quad (\text{C1})$$

In these variables Eq. (23) becomes

$$x^{1/(1-\eta)} = \beta - x, \quad (\text{C2})$$

and we assume that $\beta > 1$ (adiabatic evolutions).

A quick look at Fig. 6 makes clear that the solution can be obtained by considering a series of inequalities, numbered by index i , in the form

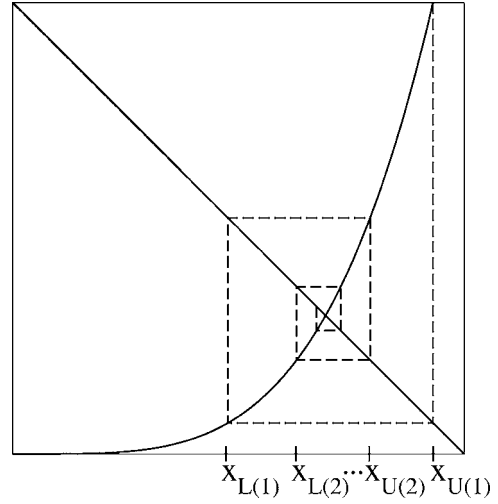


FIG. 6. Schematic plot of the recurrence method for getting the solution of Eq. (C2). Solid lines $x^{1/(1-\eta)}$ and $\beta - x$, dashed line is a construction of recurrence solutions (C3) and (C4). The plots are in a $\beta \times \beta$ box.

$$x_{L(i)} < x < x_{U(i)}, \quad (\text{C3})$$

where both lower ($x_{L(i)}$) and upper ($x_{U(i)}$) bounds satisfy the the same recurrence equation

$$x_{L,U(i)} = (\beta - [\beta - x_{L,U(i-1)}]^{1-\eta})^{1-\eta}, \quad (\text{C4})$$

with the initial conditions $x_{L(0)} = 0$, $x_{U(0)} = \beta$. Considering a few iterations one can show that the solution of Eq. (C2) can be conveniently written as

$$x^{1/(1-\eta)} = \frac{1}{(\alpha\tau_Q)^2} \left[1 - (\alpha\tau)^{2\eta} + (1-\eta)(\alpha\tau_Q)^{4\eta} + \frac{1}{2}(3\eta-2)(1-\eta)(\alpha\tau_Q)^{6\eta} + \frac{1}{3}(1-\eta)(1-2\eta) \times (3-4\eta)(\alpha\tau_Q)^{8\eta} + O(\tau_Q^{10\eta}) \right]. \quad (\text{C5})$$

Using Eq. (C5), different quantities of interest can be determined, e.g.,

$$\hat{\varepsilon}^2 = \frac{1}{(\alpha\tau_Q)^{2\eta}} \left[1 - \eta(\alpha\tau_Q)^{2\eta} + \frac{1}{2}\eta(1-\eta)(\alpha\tau_Q)^{4\eta} - \frac{1}{3}\eta(1-\eta)(1-2\eta)(\alpha\tau_Q)^{6\eta} + \frac{1}{8}\eta(1-\eta) \times (1-3\eta)(2-3\eta)(\alpha\tau_Q)^{8\eta} + O(\tau_Q^{10\eta}) \right], \quad (\text{C6})$$

$$\hat{t} = \tau_Q^\eta \alpha^{\eta-1} + O(\tau_Q^{3\eta}). \quad (\text{C7})$$

Substitution of $\eta = 1/2$ into Eqs. (C6) and (C7) reproduces adiabatic series expansions of $\hat{\varepsilon}$, \hat{t} from the standard Landau-Zener theory (7).

- [1] S. Sachdev, *Quantum Phase Transitions* (Cambridge University Press, Cambridge, England, 2001).
- [2] W. H. Zurek, U. Dorner, and P. Zoller, *Phys. Rev. Lett.* **95**, 105701 (2005).
- [3] J. Dziarmaga, *Phys. Rev. Lett.* **95**, 245701 (2005).
- [4] A. Polkovnikov, *Phys. Rev. B* **72**, 161201(R) (2005).
- [5] R. Schützhold, *Phys. Rev. Lett.* **95**, 135703 (2005).
- [6] E. Farhi, J. Goldstone, S. Gutmann, J. Lapan, A. Lundgren, and D. Preda, *Science* **292**, 472 (2001); A. M. Childs, E. Farhi, and J. Preskill, *Phys. Rev. A* **65**, 012322 (2002).
- [7] W. Wernsdorfer and R. Sessoli, *Science* **284**, 133 (1999); W. Wernsdorfer *et al.*, *J. Appl. Phys.* **87**, 5481 (2000).
- [8] I. Bloch, *Nature Physics* **1**, 23 (2005).
- [9] B. Damski, *Phys. Rev. Lett.* **95**, 035701 (2005).
- [10] T. W. B. Kibble, *J. Phys. A* **9**, 1387 (1976); *Phys. Rep.* **67**, 183 (1980).
- [11] W. H. Zurek, *Nature (London)* **317**, 505 (1985); *Acta Phys. Pol. B* **24**, 1301 (1993); *Phys. Rep.* **276**, 177 (1996).
- [12] N. D. Antunes, L. M. A. Bettencourt, and W. H. Zurek, *Phys. Rev. Lett.* **82**, 2824 (1999).
- [13] P. Laguna and W. H. Zurek, *Phys. Rev. Lett.* **78**, 2519 (1997); A. Yates and W. H. Zurek, *ibid.* **80**, 5477 (1998).
- [14] C. Bauerle, Y. M. Bunkov, S. N. Fisher, H. Godfrin, and G. R. Pickett, *Nature (London)* **382**, 332 (1996); V. M. H. Ruutu *et al.*, *ibid.* **382**, 334 (1996).
- [15] M. J. Bowick, L. Chandar, E. A. Schiff, and A. M. Srivastava, *Science* **263**, 943 (1994); I. Chuang, R. Durrer, N. Turok, and B. Yurke, *ibid.* **251**, 1336 (1991).
- [16] R. Carmi, E. Polturak, and G. Koren, *Phys. Rev. Lett.* **84**, 4966 (2000); A. Maniv, E. Polturak, and G. Koren, *ibid.* **91**, 197001 (2003).
- [17] R. Monaco, J. Mygind, and R. J. Rivers, *Phys. Rev. Lett.* **89**, 080603 (2002); *Phys. Rev. B* **67**, 104506 (2003); R. Monaco, U. L. Olsen, J. Mygind, R. J. Rivers, and V. P. Koshelets, e-print cond-mat/0503707.
- [18] C. Zener, *Proc. R. Soc. London, Ser. A* **137**, 696 (1932).
- [19] N. D. Antunes, P. Gandra, R. J. Rivers, e-print hep-ph/0504004.
- [20] N. V. Vitanov and B. M. Garraway, *Phys. Rev. A* **53**, 4288 (1996); N. V. Vitanov, *ibid.* **59**, 988 (1999).
- [21] E. T. Whittaker and G. N. Watson, *A Course of Modern Analysis* (Cambridge University Press, Cambridge, England, 1958).